

**CHARACTERIZATION OF THIN FILM PROPERTIES OF
MELAMINE BASED DENDRIMER NANOPARTICLES**

A Thesis

by

WOONG JAE BOO

Submitted to the Office of Graduate Studies of
Texas A&M University
in partial fulfillment of the requirements for the degree of

MASTER OF SCIENCE

December 2003

Major Subject: Mechanical Engineering

**CHARACTERIZATION OF THIN FILM PROPERTIES OF
MELAMINE BASED DENDRIMER NANOPARTICLES**

A Thesis

by

WOONG JAE BOO

Submitted to Texas A&M University
in partial fulfillment of the requirements
for the degree of

MASTER OF SCIENCE

Approved as to style and content by:

Roger J. Morgan
(Chair of Committee)

Richard M. Crooks
(Member)

Hung-Jue Sue
(Member)

Dennis O'Neal
(Head of Department)

December 2003

Major Subject: Mechanical Engineering

ABSTRACT

Characterization of Thin Film Properties of Melamine Based Dendrimer Nanoparticles.

(December 2003)

Woong Jae Boo, B.S., Hankook Aviation University

Chair of Advisory Committee: Dr. Roger J. Morgan

With the given information that dendrimers have precisely controlled their sizes and spherical structures in the molecular level, the aim of this study is to show that dendrimer particles can become ordered into a self-assembled regular structure due to the nature of their regular sizes and shapes. For this project, melamine based generation 3 dendrimer was used for solution cast of thin films from the dendrimer-chloroform solutions with different casting conditions, i.e. various solution concentrations, casting temperatures, and substrates. As a result of these experiments, unique phenomena of highly ordered uniform 2-D contraction separations were observed during the solvent evaporation from the dendrimer films. The cast films from the concentration of 0.8 wt% and higher exhibit regular 2-D separation contraction patterns and make well-developed regularly arrayed structures due to the interaction between the contraction stresses and adhesion strength between films and substrates. From the DSC tests, both powder and cast film samples of a dendrimer show similar melting behaviors with

different areas under the melting peaks. The results of these tests show that dendrimers, when they are in a descent environment that provides dendrimers with molecular mobility due to surface ionic bonding strength, can make a structural order and regularity in their macroscopic structures.

ACKNOWLEDGEMENTS

First, I would like to thank my advisor, Dr. Roger J. Morgan who provided me with guidance, support, and an ideal atmosphere for doing research in this group. I was able to take advantage of so many opportunities because of him. I became more independent while working with him due to his high expectations. I would like to thank my committee members, Dr. H.-J Sue and Dr. R. M. Crooks, for their commitment to this research.

Secondly, I am grateful to Erick J. Acosta and Dr. Erick E. Simanek, Chemistry Department of Texas A&M University, for supplying the dendrimer material for this project.

Finally, I would like to thank my wife, Jin Heo, for her endless support, tolerating my long absence and hard work. I also want to express gratitude and love for my father and mother in Korea for their help and support.

TABLE OF CONTENTS

	Page
ABSTRACT.....	iii
ACKNOWLEDGEMENTS.....	v
TABLE OF CONTENTS.....	vi
LIST OF FIGURES.....	viii
LIST OF TABLES.....	xi
 CHAPTER	
I INTRODUCTION.....	1
1.1 Background.....	1
1.2 Focus of Research and Goals.....	2
II LITERATURE REVIEW.....	4
2.1 General.....	4
2.2 Historical Perspective of Dendrimers.....	5
2.3 Dendrimer Construction.....	7
2.4 Applications of Dendrimers.....	13
2.5 Experimental Techniques.....	16
III CHARACTERIZATION OF THIN FILM SEPARATION PROPERTIES OF MELAMINE BASED DENDRIMER NANOPARTICLES.....	28
3.1 Introduction.....	28
3.2 Experimental.....	28
3.3 Results.....	33
3.4 Discussion.....	42

CHAPTER	Page
IV THERMAL PROPERTIES OF MELAMINE BASED DENDRIMER NANOPARTICLE.....	47
4.1 Introduction.....	47
4.2 Experimental.....	47
4.3 Results.....	51
4.4 Discussion.....	53
V CONCLUSIONS.....	59
5.1 Primary Findings.....	59
5.2 Suggestions for Future Research.....	60
REFERENCES.....	62
VITA.....	66

LIST OF FIGURES

FIGURE	Page
1	An illustration of Flory’s highly branched polymer, which is formed via trifunctional, AB ₂ -type monomers.....6
2	Illustration of preparation of dendritic polyamidoamine (PAMAM) polymers using a three-directional nitrogen core, reported by Tomalia et al.....8
3	Illustration of divergent growth of dendrimer construction, ‘P’ represents passive functionality.....10
4	Illustration of convergent growth of dendrimer construction, ‘P’ represents passive focal point.....12
5	Illustration of heating facilities and controlling units of differential scanning calorimetry.....17
6	Diagram of difference of heat flux and isothermal in DSC.....19
7	A typical DSC plot showing glass transition temperature (T _g), temperature of crystallization (T _c) and melting temperature (T _m).....20
8	Illustration of principle of AFM. A diode laser is focused onto the surface of a reflective cantilever and the laser beam is deflected off the attached cantilever into a position sensitive photodiode.....23
9	Illustration of tip broadening effect on AFM. Solid line is a real contour line of the sample and dashed line shows scanned image line under the tip broadening effect.....26
10	(a) Molecular structure of melamine based generation 3 dendrimers. (b) 3D modeling of molecular structure of the same sample material.....30
11	(a) Olympus BX60 Microscope System, (b) Detak3, Veeco Surface Profile Measuring System.....32

FIGURE	Page
12	(a) Scanning electron microscope (SEM) image of uniform 2-D contraction separation of solution cast dendrimer films on the glass substrate, sample No. 3 (0.8 wt%). (b) High magnification image of the same sample.....34
13	(a) Polarized optical microscopic image of uniform 2-D contraction separation of solution cast dendrimer films on a glass substrate, sample No. 4 (1.0 wt%). (b) High magnification, unpolarized image of same sample.....36
14	(a) Irregular crack propagation within the regularly structured blocks of the solution cast film with a high concentration of dendrimer, sample No. 5 (2.0 wt%). (b) High magnification image of the same sample.....37
15	Optical micrographs of difference of contraction separation patterns due to the temperature effect over solution cast films. (a) Sample No. 4a, (1.0 wt%) at 25°C, (b) sample No. 4c (1.0 wt%) at 60°C.....38
16	(a) Surface profile of a regularly separated single block, sample No. 3 (0.8 wt%). (b) Illustration of comparison of the solvent evaporation sites.....40
17	(a) Surface profile of solution cast thin film of melamine based generation 3 dendrimer, sample No. 3 (0.8 wt%), 4 (1.0 wt%), and 5 (2.0 wt), (b) near the center, irregularity of cracking behavior is higher than periphery of cast film, sample No. 5 (2.0 wt%).....41
18	Schematic representation of contraction separation in solution cast film. Discontinuity of tangential separation explains that contraction separation developed in (a)radial direction prior to (b)tangential separation.....44
19	(a) Digital Instruments Nanoscope AFM/STM for scanning probe microscopy system. (b) Monitor screen image of scanning cantilever on a regularly cracked dendrimer film sample, (Tip Width ~ 80µm).....50
20	DSC curves of melamine based dendrimers in powder and cast film. The cast film curve is shifted vertically.....52

FIGURE	Page
21	AFM result image from solution cast G3D dendrimer film before annealing. Maximum data scale in Z-direction is $\pm 2.5\text{nm}$54
22	(a) AFM result image from solution cast G3D dendrimer film after annealing (100°C , 2 hours). Maximum scale in Z-direction is $\pm 2.5\text{nm}$. (b) Cross sectional view of A-A on image (a).....54
23	Polarized light image of sample No. 4 (1.0 wt%). The bright areas exhibit birefringence under the polarized light from the light source due to the stress-induced order.....57
24	An ideal schematic model of close packed elliptic sphere molecules on a substrate. Δh represents the thickness of first monolayer.....58

LIST OF TABLES

TABLE		Page
1	Samples with various concentrations for solution cast thin film property tests.....	31
2	Thermal properties of melamine based dendrimers determined by DSC.....	52

CHAPTER I

INTRODUCTION

1.1 Background

Since dendrimer chemistry was first introduced in the late 1970s, dendritic polymer synthesis has developed rapidly and become one of the fastest growing areas of interest in polymer science with its unique molecular structural properties. As is well known, the dendrimer has a globular structure in which well-defined branches radiate from a single central atom or groups of atoms. The central core forms the first generation of branches, and becomes more branched and dense as they extend outward generation by generation. Some of the largest dendrimers have a diameter of more than 10 nm. These unique globular molecules have great potential in a number of applications as a result of the high degree of surface functionality, the presence of nano-scale cavities within the structure, and the precisely controlled molecular sizes [1-5].

Dendrimers are of interest in a variety of fields, such as host-guest chemistry and catalysis in which the core region, which is usually highly porous, can exhibit interesting host behavior, while densely packed outer layers act as shield layers for the

interior regions from the surrounding medium. This suggests applications in mimicking the hydrophobic pocket regions in enzymes. In medicine, the feature of an outer surface which is composed of multiple identical binding sites is potentially important in pharmacology because of amplified substrate binding [6]. Dendrimers could also be important in the context of functional materials and the construction of structured molecular devices for applications in fields such as light-harvesting technology [7]. In addition, highly controlled and well defined layer-by-layer structures, and the narrow molecular weight range, i.e. monodispersity, of dendrimers make their behavior easier to characterize than polymeric materials.

Although, most of the dendrimer research to date has been focused on their synthesis, chemical properties and molecular structural characteristics, investigations and researches on the physical properties and structure-property relationships of dendrimers [8] are beginning to emerge. Recently studies on the physical properties, (i.e., surface tension and pressure of radially layered copoly(amidoamine-organosilicon) (PAMAMOS) dendrimers [9]), and properties of dendrimer-based films, sheets and membranes [10], and structure-property relationships in conjugated molecules [11], have been conducted and published.

1.2 Focus of Research and Goals

From studies to the 1990's, it had been known that dendrimers do not form 3-D crystalline structures despite their regular size and spherical structure [12]. However,

crystalline and liquid-crystalline structures of disk-like triphenylene monomers have been characterized by Vogit-Martin et al. [13] and a study about the diffraction patterns of crystalline dendrimers was reported by Bunchko et al. [14].

Also some possibility of relatively stiff dendrimers available to form a regular structure and/or order at macroscopic ranges has been reported from the studies on preparation of dendrimer monolayers [15, 16], and dendrimer multilayers [17-19]. From this previously published work, it might be expected that using dendrimers which are well controlled in size and well defined in surface groups, will enable control of nano-scale order in the polymer films, membranes, and even matrices.

In this study, several physical properties of melamine based, generation 3 dendrimer in the form of powder and solution cast thin film are investigated to observe whether or not structural order in microscopic and macroscopic ranges occurs. The final aim of this study is to show that dendrimers or other spherically structured nano-scale particles can become ordered into a self-assembled regular structure due to the nature of their regular sizes and shapes. This would mean that one of the most important physical properties of dendrimers, can lead to regularly arrayed self-assemblies during processing.

This study shows the unique phenomenon of regular contraction separation of solution cast films made from generation 3 melamine based dendrimers and their thermal properties.

CHAPTER II

LITERATURE REVIEW

2. 1. General

The name “dendrimer” is originated from Greek words “dend-” meaning “tree” and “-mer” meaning “part” from Greek, describes the new type of structural architecture of this 3-dimensional molecule. Although the first name “cascade molecule” is more suitable to describe dendrimers’ own 3-D feature, [20] the name “dendrimers” has been used widely. The synthesis and chemistry of dendrimers are relatively new fields of polymer chemistry which are defined by regular and highly branched monomers building up to a monodisperse, tree-like-branched structures [21].

Synthesis of this type of monodisperse polymers demand a highly precise synthetic control which is achieved through stepwise reactions, building the dendrimer up one monomer layer, called "one generation," at one synthesizing step. Each dendrimer is composed of a center core molecule which has multifunctional sites with a dendritic wedge attached to each functional site. Usually the core molecule is called as ‘generation 0’. Each continuous repeat unit along all functional branches builds the next generation, ‘generation 1’, ‘generation 2’, and so on, until the synthesizing steps reach the outmost generation. [22]

2. 2. Historical Perspective of Dendrimers

The history of the dendritic macromolecules can be dated back to 1941 when Flory first published papers which were describing the gelation phenomenon [23-25]. The term ‘gel’ meant to describe only those polymeric materials that were insoluble in all solvents, as opposed to the term ‘sol’, which meant the soluble polymeric materials [26]. By Flory’s work, the experimental evidences for formation of branched-chain, three-dimensional macromolecules in polymerizations were provided.

In 1952, Flory provided new evidence to prove that highly branched polymers could be polymerized without the occurrence of gelation by using a trifunctional monomer that possesses two different functional groups (A and B) [27]. The illustration of a highly branched polymer that is built by reacting a monomer of the type AB_2 is shown in Figure 1. Vogtle et al. first reported the preparation, separation, and characterization of dendritic molecular structures with branched topologies through iterative methodology in 1978 [20]. He described “cascade syntheses” as “reaction sequences which can be performed repeatedly.”

By 1982, Maciejewski and other chemists began to give consideration to applications for dendritic macromolecules [28]. His publication on “Trapping Topologically by Shell Molecules” described the phenomenon of dense packing, and to explain topology of cascade polymers. Due to his theory, a cast cascade polymer molecule could trap solvent molecules (or guests) within its infrastructure. He also demonstrated the synthesis of cascade polymers of cylindrical topology, which could

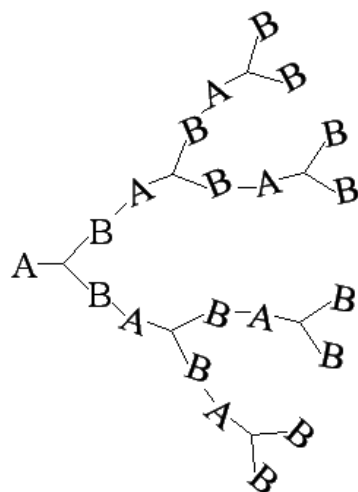


Fig. 1. An illustration of Flory's highly branched polymer, which is formed via trifunctional, AB_2 -type monomers [27].

be synthesized by selecting an interactive synthesis that began with a linear, long-chain polyfunctional core, such as polyvinylamine [28].

In 1985, two major macromolecule research groups, Newkome's and Tomalia's (Dow Chemical) announced their works dealing with cascade syntheses. Newkome [29-31] had developed a series of highly branched molecules to acquire the higher degree of surface functionality, where each generation had a different constitution. These molecules were called "arborols" (arbor; Latin for "tree"). The research of Tomalia et al. [32] concentrated on the synthesizing of dendritic polyamidoamine (PAMAM) polymers employing a three-directional nitrogen core, as illustrated in Figure 2.

The structure of poly(amidoamines) (PAMAMs) contains a three-directional ammonia core, nitrogen three-directional centers for branching units, and C-N bonds formation for monomer connectivity as shown in Figure 2. Tomalia titled his polymers as 'starbust dendrimers'. After this early stage of research of macromolecular chemistry, dendritic polymer synthesis has developed rapidly and become one of the fastest growing areas of interest in polymer science.

2. 3. Dendrimer Construction

Most syntheses of dendrimers, generally, contain the repetitious and alternative steps of a growth reaction and an activation reaction. These reactions must be performed at many sites in a molecule simultaneously the dendrimer synthesizing steps.

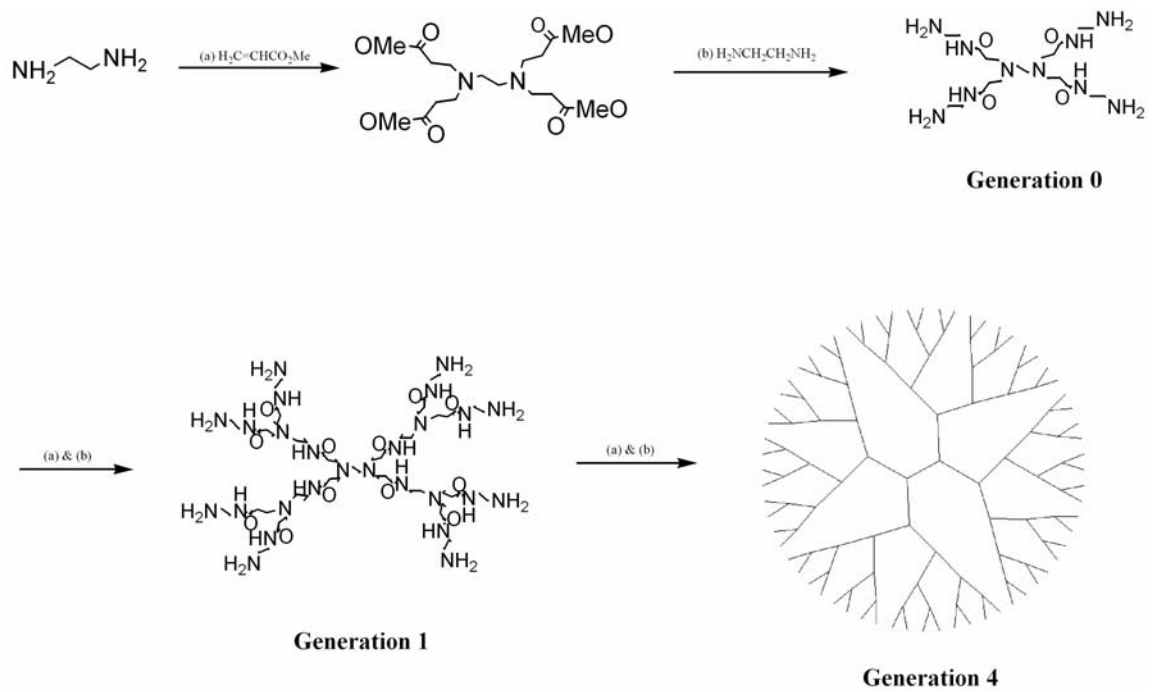


Fig. 2. Illustration of preparation of dendritic polyamidoamine (PAMAM) polymers using a three-directional nitrogen core, reported by Tomalia et al. [3, 4, 32].

Particularly, the whole process must be controlled very 'precisely'. There are two major methods for dendrimer synthesis: the divergent growth method and the convergent growth method.

2.3.1 Divergent Growth Method

Divergent growth method needs two main steps: One is the activation of the functional groups on the sites and the other is the attaching of branching monomer units on those sites that were activated previously [33]. The reaction starts at the reactive sites of the core and continues to the periphery, as shown in Figure 3. To the initial monomer (core), which possesses one or more reactive sites, a layer of monomer is covalently connected and builds a generation.

The core material possesses several reaction sites initially. The first generation monomer units react with the core readily. Once all reactive sites are taken by the monomer units and the additive reaction stops, the end groups of the previously added branch units must be activated to start further reaction.

Then additional monomers are attached on those activated sites of the molecules again and form a new generation. Polymer growth in this manner, from inside to the out side is named as 'divergent' synthesis. By this synthesizing manner, the structure and molecular weight of dendritic molecules can be controlled precisely. In recurrent generation growing reactions, side reactions and incomplete additions

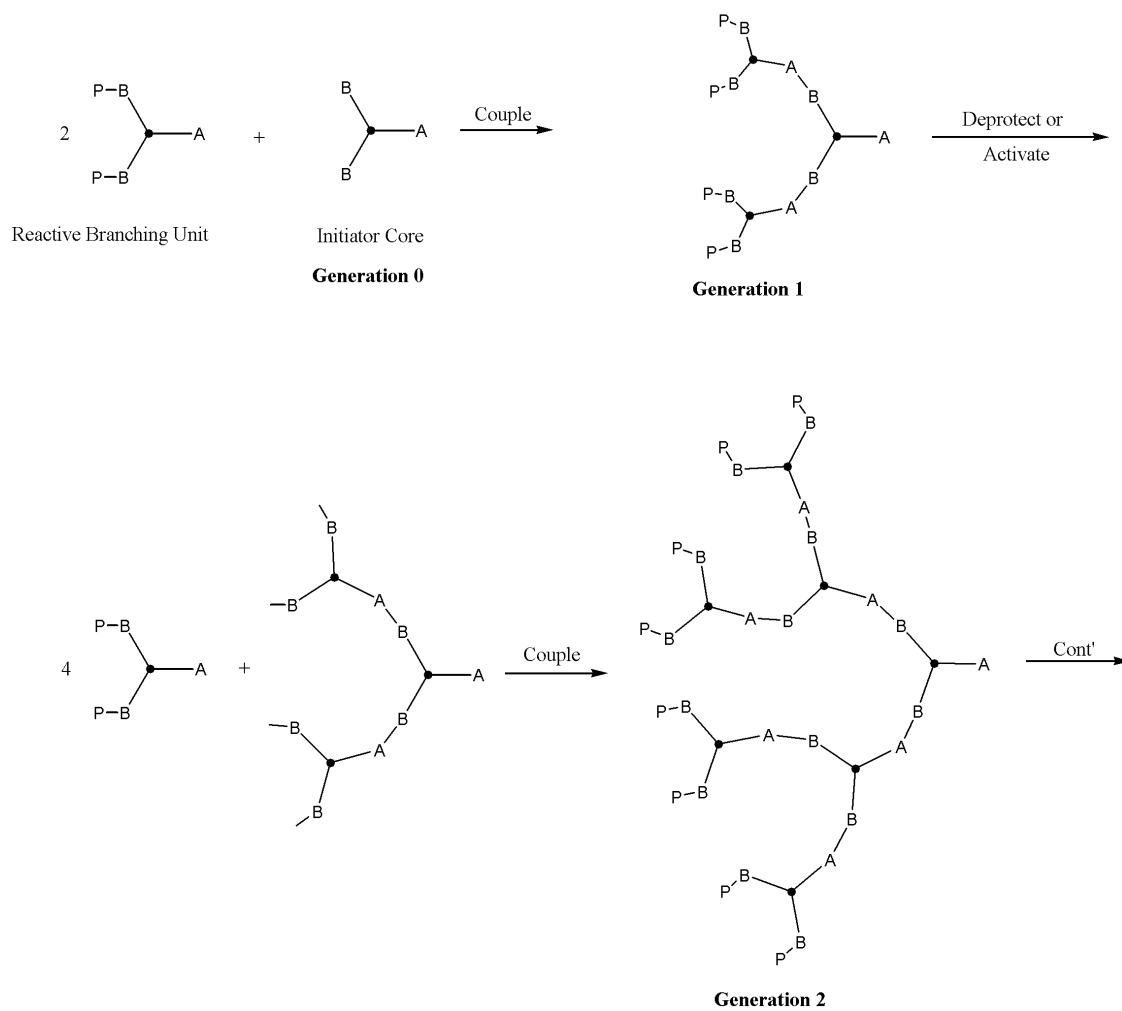


Fig. 3. Illustration of divergent growth of dendrimer construction, 'P' represents passive functionality [3, 4, 32].

become more apparent [33]. Sterical hindrance of monomers which are branched out is one of the main reasons for defect formation and the disadvantages of the divergent growth method. In each reaction step, the overall amount of yield is small, and the products must be purified.

However, one of the advantages of this method is the ability to modify the whole surface of the dendrimer molecule. By changing the surface groups at the outermost generation, the overall chemical and physical properties of the whole synthesized material can be changed and controlled for specific needs [32, 34, 35]. This versatility of dendrimer synthesis is one of the main reasons of high interest in dendrimer research. Tomalia's PAMAM dendrimers were synthesized by this divergent method, starting with an initiator core and branching out to the surface of the dendrimer [35].

2.3.2 Convergent Growth Method

Another main dendrimer synthesis method is the convergent growth method employing the strategy that polymeric branches are grown from the outside to the inside. The concept is illustrated in Figure 4. One of the disadvantages of divergent growth method is that the dendrimer has only one kind of surface functional group. This kind of demerit can be eliminated by the convergent growth method.

The convergent growth method was first presented by Frechet [36]. The reaction starts at the surface units of the dendrimers and proceeds toward the inside and

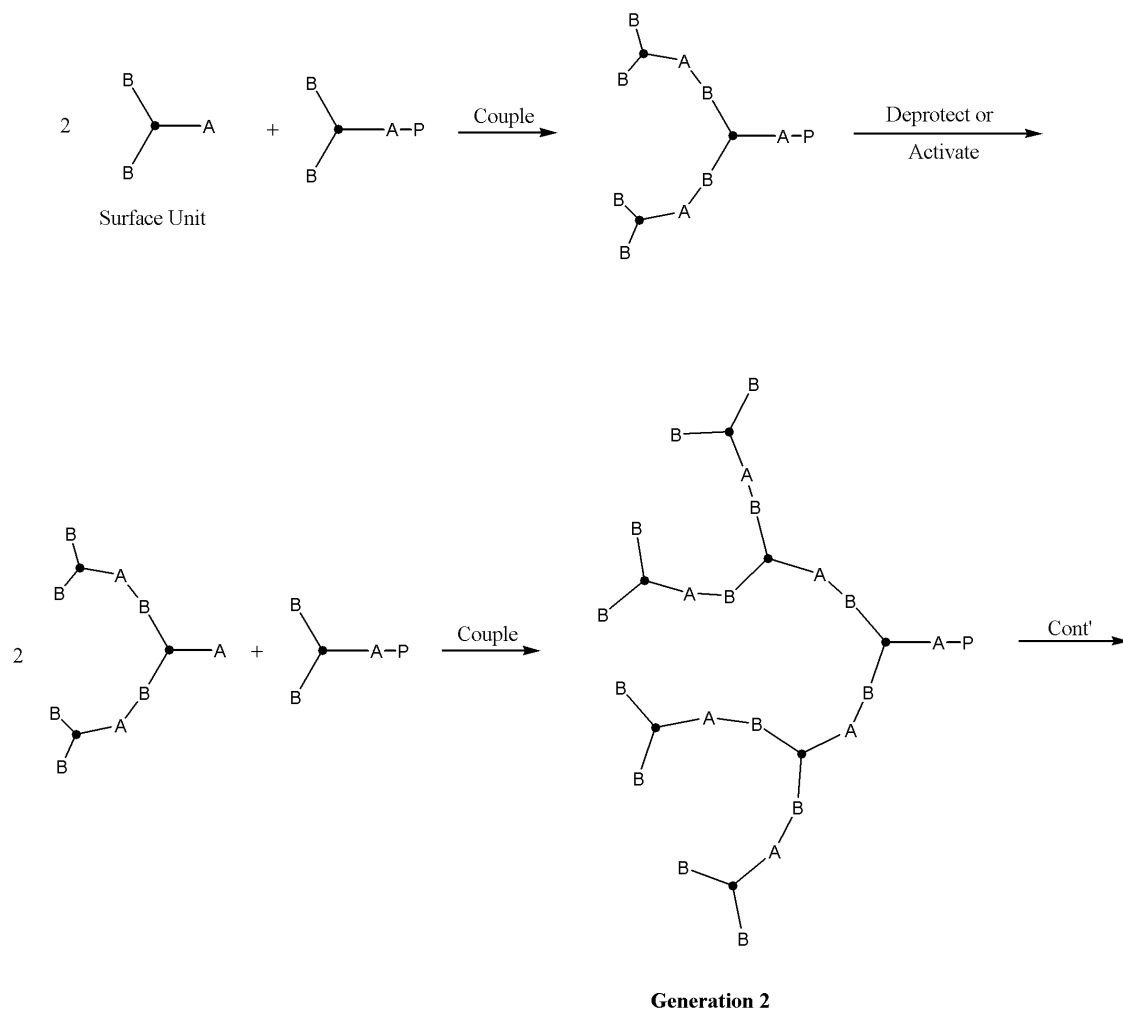


Fig. 4. Illustration of convergent growth of dendrimer construction, 'P' represents passive focal point [3, 4, 32].

finally reaches to the core. Like the divergent growth method, this reaction is also composed of two steps: the activation and the attachment. The structural units before the final attachment to the core are called the 'wedge'. Usually, three or four wedges attach to the core and build a dendrimer molecule. Each wedge can contain different surface functional groups at their surface, and this allows that the synthesis of unsymmetrical dendrimers is possible.

Except for these two synthesis methods mentioned above, the combination of these two methods can be used to tailor for special properties. The two strategies provide associative choices for dendritic polymer synthesis. In some cases, a convergent-divergent strategy may be desirable. Hence, the appropriate choice of the synthesis method is one of the most important factors for dendrimers' chemical and physical properties, as well as selection of initial core and building block materials.

2. 4. Applications of Dendrimers

As mentioned in Chapter I, dendritic macromolecules are unique types of polymers which play an important role in emerging nanotechnology. Due to their tree-like, spherical molecular structure, they maintain high surface functionality which makes them useful as a catalyst, building blocks and carrier molecules at the nanoscale range. Dendrimers also play important role in traditional technologies such as coatings, as the spherical molecular structure expresses unique viscosity characteristics. Whether used in state-of-the-art modern nanotechnology or traditional usages, dendrimers are

synthetically versatile and flexible in their applications. The following are some areas of the successful applications of dendrimers that were used as sample materials in this research.

2.4.1 Dendrimers as Building Blocks for Surface Modifications

Self-assembled monolayers made from dendrimers, which have a well-developed three dimensional structure and a large number of surface functionalities, may show improved substrate adhesion and stability when they are compared to molecules of two-dimensional structure [17, 19]. As a potential material for surface modification, dendrimers also have an advantage over conventional linear polymer films as they can be used to form highly crosslinked thin films with many film-surface functional groups for additional bonding applications [19].

2.4.2 Applications in Medicine and Biology

Other successful applications of dendrimers are medicine and biology fields. Due to the capability of hosting small organic molecules, dendrimers have been used as drug delivery systems [37], which is essential to transport biological molecules to the required site. As a contrast agent for magnetic resonance imaging (MRI), PAMAM dendrimers have been used to visualize the blood stream in the body, and to help to diagnose disease in an organ [38]. In addition to these examples, many dendrimer-

based biomolecules have been synthesized by functionalization of the dendrimer surface with different biologically active molecules.

2.4.3 Dendrimers as Catalysts

The nature of the polyvalency of dendrimers offers their application as frames which provide the places where catalytic sites are attached. The higher functional groups of dendrimers can be utilized to advantage in many ways for catalyst applications [38]. The internal cavity of dendrimer molecules allows many new possibilities for catalyst design. For example, a metal cluster may be grown and trapped inside the cavity of dendrimers [39].

2.4.4 Dendrimers as Controlling Agents in Energy and Electron Transfer

The structure of a dendrimer is topologically ideal for being used as a molecular antenna, which is an arranged collection of chromophores that collects, directs, and transfer electromagnetic energy [40, 41]. A large number of chromophores at the surface of a dendrimer molecule can absorb radiation and lead it to successively fewer chromophores in interior regions of the dendrimer by an energy transfer mechanism. Topologically, the structure of dendrimers allows the most efficient way of gathering a set of chromophores for energy collection and transfer.

Except for the applications mentioned above, there are a number of other areas where dendrimers have been used and show their advantages. For example, Lakowski et al. reported patterned surface layers with micrometer-sized features by micro contact printing in 1999 [42], and applications of dendrimers in the photoresist areas have recently emerged [43]. These applications utilize the unique properties of dendrimers in lithography and other electro-chemical device constructions. With these active areas of the dendrimer applications, a number of additional applications are expected in the near future.

2. 5. Experimental Techniques

2.5.1 Differential Scanning Calorimetry (DSC)

Differential scanning calorimetry (DSC) is one of the most widely used techniques for thermal characterization of material properties. It is used to study the thermal transitions of materials. In a DSC, a sample and an empty reference are thermally compared in small aluminum pans with crimped covers. Both sample and reference pans are placed on individual heaters in the furnace in a nitrogen atmosphere. A diagram of DSC heating chamber and a control system is shown below, Figure 5.

DSC has two independent heating chambers, one for the sample and the other for reference. Each chamber is built on a temperature-controlled heater and the temperatures of the two chambers are monitored and controlled continuously. The

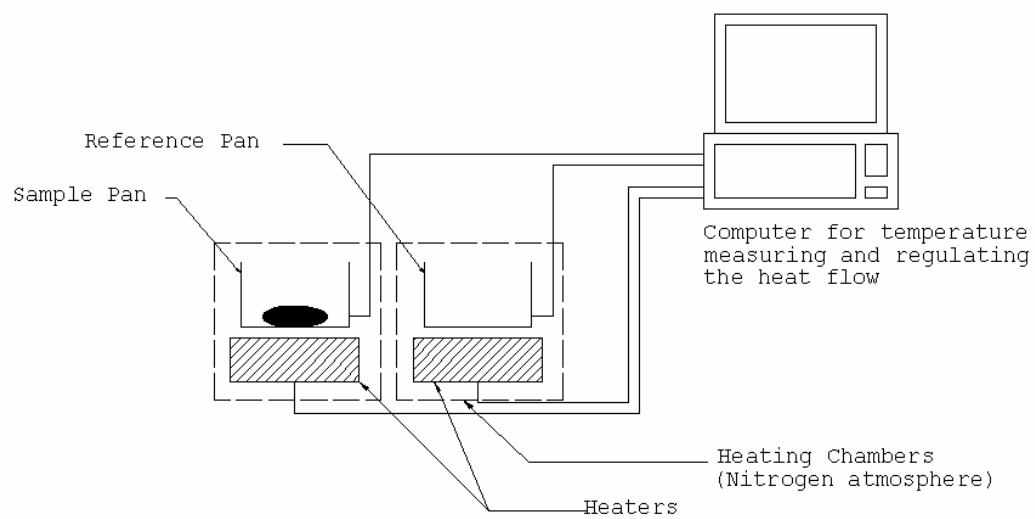


Fig. 5. Illustration of heating facilities and controlling units of differential scanning calorimetry.

output information from each chamber is transferred through a differential amplifier and analyzer in a control computer.

An amplifier adjusts the power output to the each chamber to maintain the same temperature in both chambers (isothermal, as in Figure 6), i.e.

$$\Delta T = T_s - T_r = 0,$$

where, T_s is the sample pan temperature,

T_r is the empty reference pan temperature.

The heat flux difference between sample and reference is observed and plotted on the computer screen as a function of temperature or time. When the sample material reaches at the thermal transition temperature, such as glass transition temperature (T_g), a plot, as shown in Figure 7, can be obtained. There is a sudden change in heat capacity at the glass transition temperature (T_g) as more heat can be absorbed due to greater molecular motion per 1oC rise in temperature [44, 45].

When sample materials, for instance polymers, reach a certain temperature above the T_g , they have enough energy to orient themselves into crystalline structures. To form crystal structures, polymers radiate heat. Therefore the heat flow to the sample pan is reduced to keep isothermal in the whole system. The DSC plot shows the heat given out by the material plotted down as a dip, as shown in Figure 7. This temperature is called the crystallization temperature (T_c) at which crystallization takes place. Since heat is radiated from the material, it is called an exothermic transition.

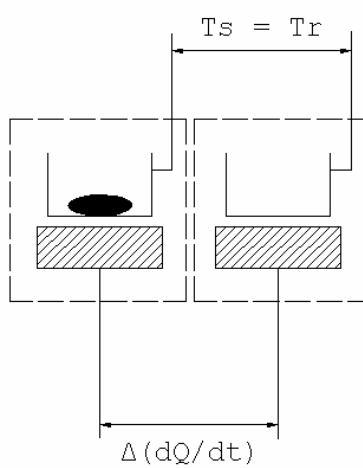


Fig. 6. Diagram of difference of heat flux and isothermal in DSC.

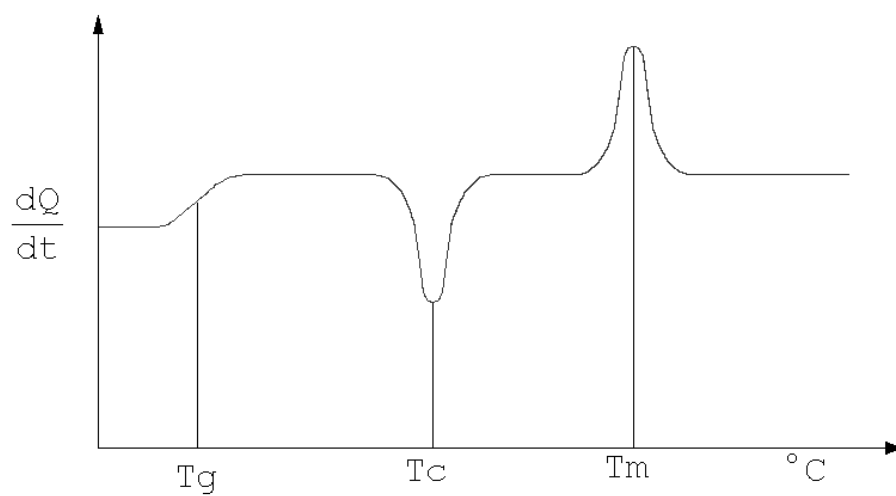


Fig. 7. A typical DSC plot showing glass transition temperature (T_g), temperature of crystallization (T_c) and melting temperature (T_m).

To dissociate the crystal structures of a material, the sample has to absorb heat from the heater and the temperature at which this takes place is called the melting temperature (T_m) and plotted up as a peak on the DSC screen. Since heat is absorbed it is called an endothermic transition. The requirements for the reference material are that it must not undergo any thermal transition over the experiment temperature range, the heat capacity and the thermal conductivity of the reference material should be similar to the sample. Empty aluminum pan is often used as a reference for thermal property characterization of polymers. Aluminum sample pans and holders are usually used up to 500°C.

2.5.2 Atomic Forced Microscopy (AFM)

In 1985, the first Atomic Force Microscope (AFM) was made by Binnig, Quate and Gerber [46] using the cantilever systems to examine the surface profile of insulating surfaces. A sharp and small needle attached at the end of the vibrating cantilever was pressed against the surface while the surface area of the sample was scanned beneath the tip. The main objective of the operation of the AFM is to measure the forces between a sharp probing tip and the surface of the sample at the micro, nano and molecular level. Images are captured by scanning the sample relative to the scanning tip and measuring the deflection of the cantilever as a function of lateral position. Owing to very small forces used for the probing tip, non-destructive scanning is possible with these small forces [47].

The first AFM used a scanning tunneling microscope at the end of the probing cantilever to detect the amount of bending of the lever. However, most AFMs use an optical lever technique recently. A sharp tip which is bonded beneath the vibrating cantilever is scanned over an objective surface of the sample with feedback mechanisms. This mechanism allows the piezo-electric scanners to maintain the force or height of the tip at a certain constant over the entire objective sample surface. Tips are typically made from Si_3N_4 or Si, and stretched down from the end of a cantilever. The nanoscopic AFM head employs an optical detection system in which the tip is attached to the underneath of a laser-reflective cantilever. A diode laser is focused onto the surface of a reflective area at the end of the cantilever, as shown in Figure 8. As the tip underneath the cantilever scans the objective surface of the sample, moving up and down with the contour of the surface, the laser beam is deflected off by the moving cantilever into a photodiode. The position sensitive photodetector measures the difference in light intensities, and then converts it into voltage. Via control system from the computer, feedback from the photodiode difference signal enables the tip to maintain either a constant force or constant height above the sample.

The methods for obtaining contrast image can be achieved in many ways. The following three main classes of interaction are contact mode, tapping mode and non-contact mode. In this research, tapping mode AFM was used for imaging of surface profile of a solution cast dendrimer film and discussed in Chapter IV.

The contact mode is the most common method of operation of the AFM. The tip and sample maintain the close contact as the scanning proceeds. The tapping mode

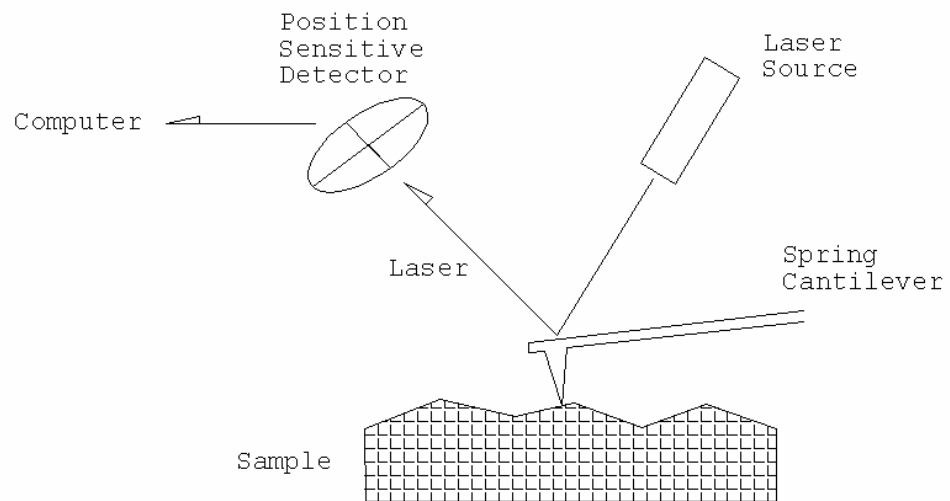


Fig. 8. Illustration of principle of AFM. A diode laser is focused onto the surface of a reflective cantilever and the laser beam is deflected off the attached cantilever into a position sensitive photodiode.

is the next most common mode used in AFM. When operated in air or other gases, the cantilever is oscillated at its resonant frequency and positioned above the surface so that cantilever taps the surface only for a very small fraction of its oscillation period. This is still contact with the sample in the sense defined earlier, but the very short time over which this contact occurs means that lateral forces are reduced as the tip scans over the object sample surface. When very soft or poorly immobilized samples are scanned, the tapping mode is better choice than the contact mode for a better result of scanned image. Other types of image obtaining are also possible with the tapping mode. In the constant force mode, the feedback adjusts the force of the vibration of cantilever, so that the amplitude of the cantilever oscillation maintains a constant.

An image can be obtained from this amplitude signal, as there will be small variations in this oscillation amplitude due to the control electronics not responding instantaneously to changes on the specimen surface. Recently, there has been much interest in phase imaging. This obtains scanned images by measuring the phase difference between the oscillations of the cantilever driving piezo and the detected oscillations. The image contrast is derived from image properties such as stiffness and viscoelasticity of the surface of the samples.

The other method is the non-contact mode. The cantilever must be oscillated above the surface of the sample at such a distance that there is no longer a repulsive force of the inter-molecular force curve. This non-contact mode AFM is a very difficult to operate in ambient conditions. The thin layer of water contamination which might exist on the surface of the sample will build a small water bridge between the tip and

the sample by the capillary force, and then this capillary effect leads the tip to 'jump-to-contact' phenomenon. Even under liquids and in vacuum, jump-to-contact phenomenon is not easy to avoid.

The sharpness of the probing tip attached the vibrating cantilever is one of the most important factors in influencing the resolution. The best tips may have a radius of curvature of only around 5nm. The importance of tip sharpness is normally explained in terms of tip convolution. This term is often used to describe all influence of the tip sharpness during the scanning process. The main influences are interaction forces, compression, broadening, and aspect ratio [46]. When the radius of curvature of the tip is similar with or greater than the size of the feature to be imaged on the objective surface, the tip broadening effect increases. Figure 9 illustrates this problem. As the tip scans over the sample, the advancing sides of the tip make contact before the end of the tip, and the microscope begins to respond to the feature. This is also called tip convolution.

Compression occurs when the tip is right over the sample to be imaged. It is difficult to determine in many cases how important this affect is, but in the studies on some soft biological polymers or in the studies of measuring in nanometer range, this effect should not be overlooked. Even though interaction forces between the tip and sample are the reason for image contrast with the AFM, some changes may be due to a change in force interaction. Forces due to the chemical nature of the tip are probably most important here, and selection of a particular tip for a particular sample material

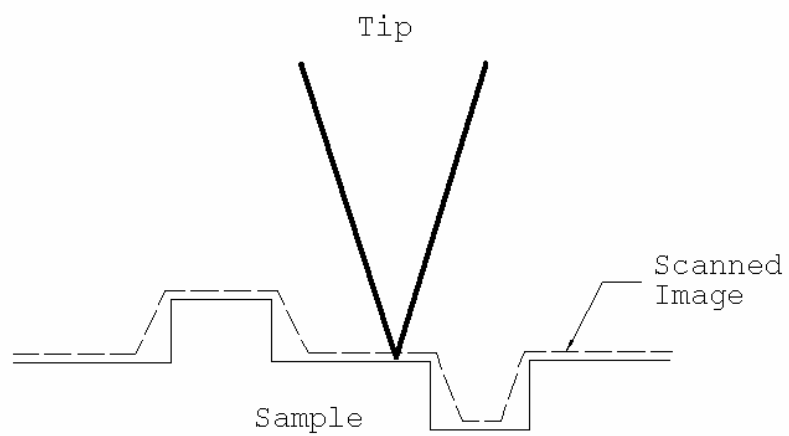


Fig. 9. Illustration of tip broadening effect on AFM. Solid line is a real contour line of the sample and dashed line shows scanned image line under the tip broadening effect [46].

can be important. Chemical mapping employing specially treated or modified tips is another important factor of current research in AFM.

The aspect ratio, which is also called the ‘cone angle’, of a particular tip is very critical when we scan the samples which have steep sloped features. Electron beam deposited tips has been used to image steep-walled features far more faithfully than can be achieved with the common pyramidal tips. In this study, general pyramidal tips were used since the scanning area were mainly situated on the top surface on the sample bodies.

CHAPTER III
CHARACTERIZATION OF THIN FILM SEPARATION
PROPERTIES OF MELAMINE BASED DENDRIMER
NANOPARTICLES

3. 1. Introduction

In this chapter, unique physical phenomena of melamine based, generation 3 dendrimer, when they form a film from solution casting, are investigated to observe whether or not structural order at the nano, microscopic, and macroscopic scale ranges occurs. The purpose of this experiment is to show that dendrimers or other spherically structured nano-scale particles can become ordered into a self-assembled regular structure due to the nature of their regular sizes and shapes. This would mean that one of the most important physical properties of dendrimers, homogeneous size and shape, can lead to regularly arrayed self-assemblies during processing, as stated in Chapter I.

3. 2. Experimental

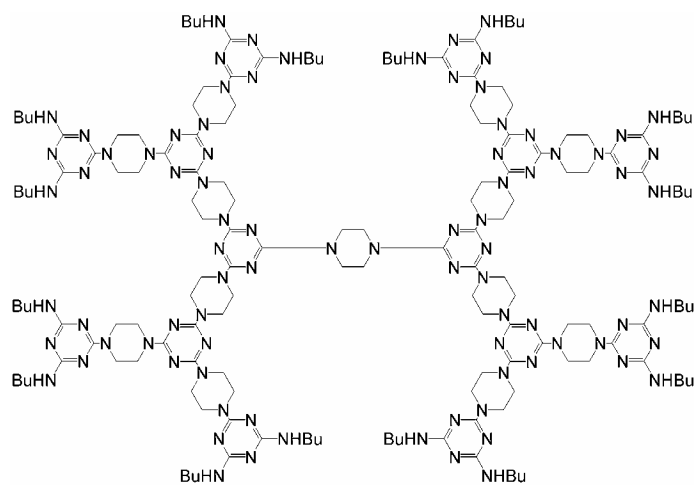
3.2.1 Material

Melamine based generation 3 dendrimer, molecular weight 3,340 was obtained from the Department of Chemistry, Texas A&M University. This material had been

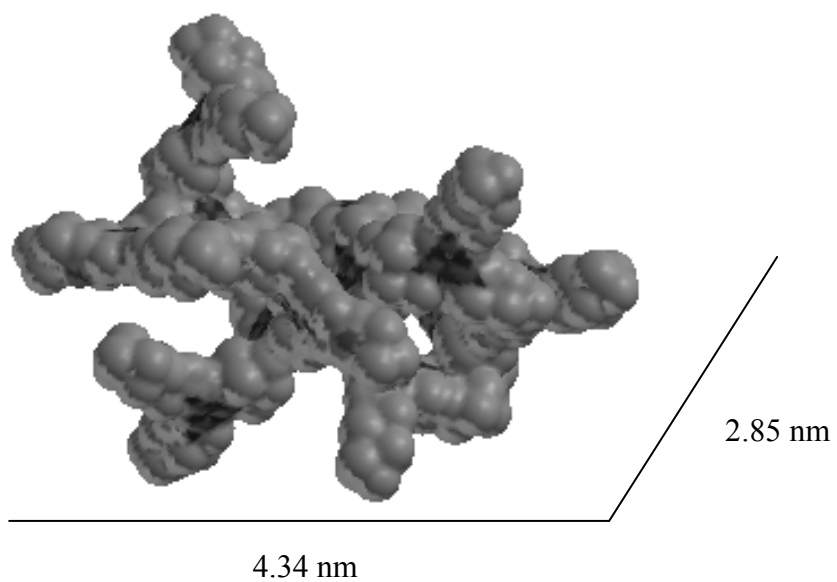
synthesized according to the literature [48], and dried in a vacuum oven at 25°C for 24 hours. Figure 10 illustrates the material structure of this dendrimer. The reagents used in processing were obtained from Aldrich.

3.2.2 Solution Cast Film Properties

The solutions of melamine based, generation 3, dendrimer and chloroform were accurately measured and prepared in from 0.3 to 2.0 wt% concentrations as shown in Table 1. Small quantities of each solution were carefully dripped onto substrates: glass, aluminum, copper, and polyethylene. The solutions on the substrates were evaporated at 25°C for 24 hours to remove chloroform. To understand the temperature effect for dendrimer solution casting, solutions of 1.0 wt% were dripped onto the glass substrates whose surface temperatures were 25°C, 40°C, and 60°C, shown in Table 1, sample 4a, 4b, and 4c, respectively. Optical microscopy was performed using an Olympus BX60 Microscope System. Scanning electron microscopy (SEM) was carried out with an Electroscan ESEM E-3 System. For optical microscopy and SEM tests, microscope cover glasses were used as substrates for solution cast films. For the surface profile and thickness variation of the cast thin films, surface profile measuring tests were carried out at room temperature in a dust free space on a Dektak 3, Veeco Surface Profile Measuring System as shown in Figure 11.



(a)



(b)

Fig. 10. (a) Molecular structure of melamine based generation 3 dendrimers [48]. (b) 3-D modeling of molecular structure of the same sample material.

Table 1.

Samples with various concentrations for solution cast thin film property tests.

Sample No	Phase	Concentration (wt%)	Substrate Temperature (°C)
1	Solution	0.3	25
2	Solution	0.4	25
3	Solution	0.8	25
4a	Solution	1.0	25
4b	Solution	1.0	40
4c	Solution	1.0	60
5	Solution	2.0	25
6	Powder	100	—



(a)



(b)

Fig. 11. (a) Olympus BX60 Microscope System, (b) Detak3, Veeco Surface Profile Measuring System.

The surface of the circular dendrimer film was scanned in the radial direction. The surface profile of separated film blocks was scanned in the tangential (X-X) and radial (Y-Y) directions to determine where regular contraction separation had occurred.

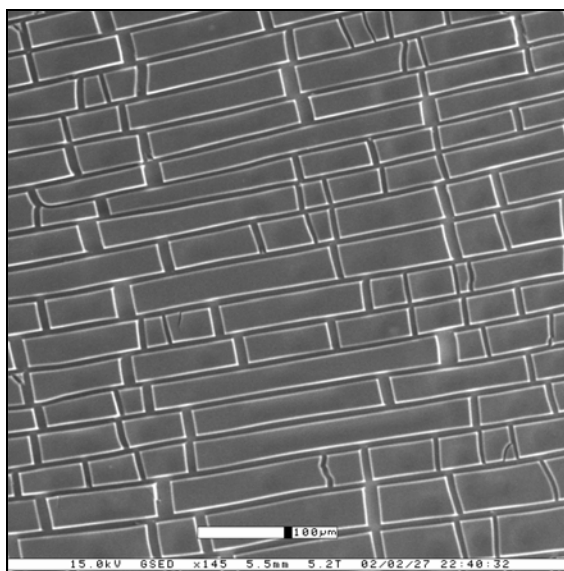
3.2.3 Small Angle X-ray Scattering (SAXS)

The solutions of melamine based generation 3 dendrimers, whose concentrations were 0.8w% and 1.0 w%, were cast on Al₂O₃ wafers at room temperature for the small angle X-ray scattering test. After 24 hours drying, the film samples were placed on the sample holder of the small angle X-ray scattering equipment, D/MAX-RAPID microdiffraction system. Data collecting period was 2 hours for each sample.

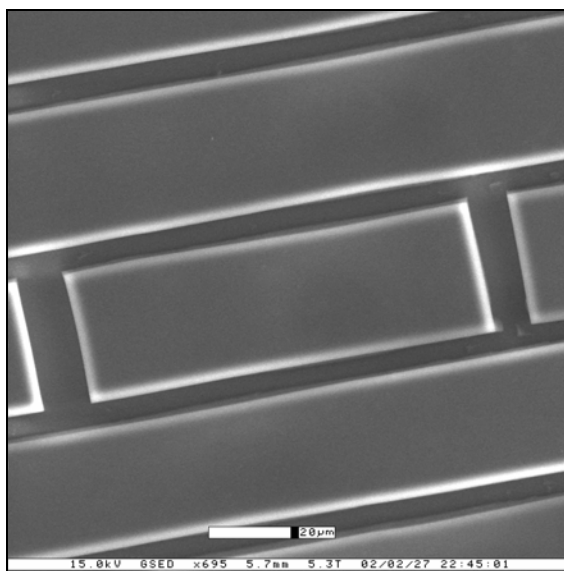
3.3. Results

3.3.1 Uniform 2-D Contraction Separation Phenomena

When various concentrations of solutions, as shown in Table 1, were used for casting of thin films on the microscope cover glasses, the cast films exhibited uniform 2-D contraction separations right after evaporation of the solvent as shown in Figure 12. The same pattern of contractions also occurs on aluminum, copper, and polyethylene substrates. While no right-angled uniform contraction separation was observed in the



(a)



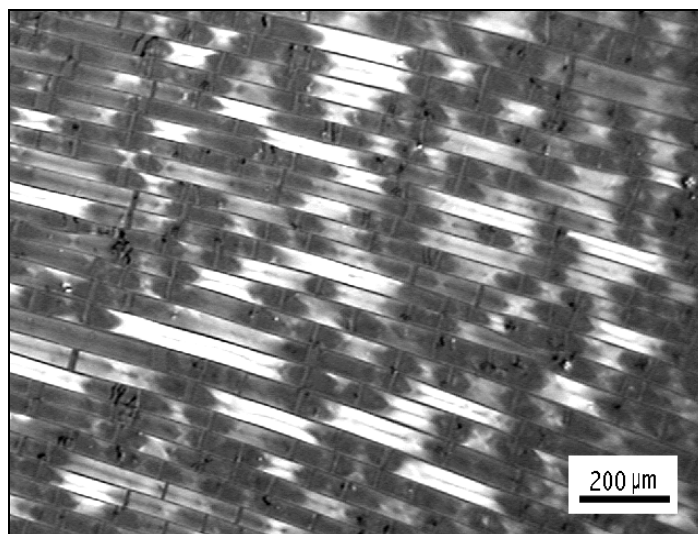
(b)

Fig. 12. (a) Scanning electron microscope (SEM) image of uniform 2-D contraction separation of solution cast dendrimer films on the glass substrate, sample No. 3 (0.8 wt%). (b) High magnification image of the same sample.

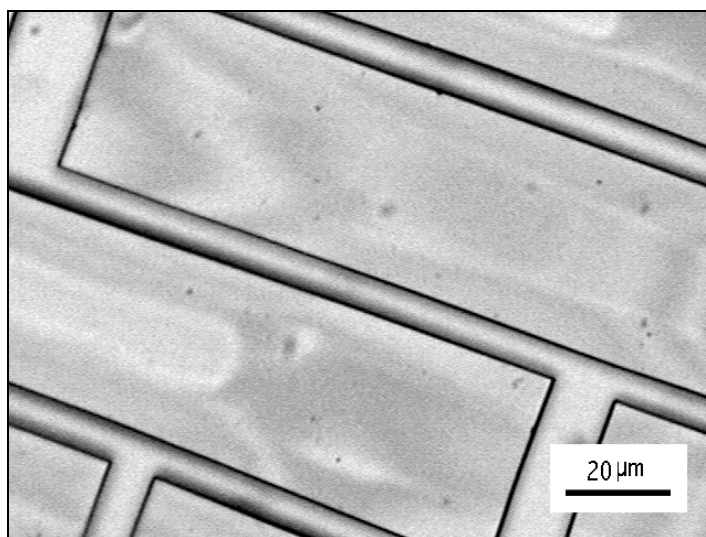
thin film cast from sample 1 (0.3 wt%), several were observed in sample 2 (0.4 wt%), and uniform 2-D contraction separations were well developed in sample 3 (0.8 wt%) and 4 (1.0 wt%), as shown in Figures 12 and 13. The tendency of right-angled uniform contraction seems to increase with the concentration of the dendrimer solution.

Sample No 5 (2.0 wt%), which has twice the dendrimer concentration of sample No.4 (1.0 wt%), exhibits a different structural separation pattern. The film from sample No. 5 (2.0 wt%) also has regular patterns in its contraction separation structures, however additional irregular crack propagations are also observed as shown in Figure 14. After experiencing of the regular contraction separations, which are observed in the cast film from sample No 4, irregular secondary cracks, often spiral in geometry, were developed in the previously separated regular block structures, shown in Figure 14.

For the effect of variation of evaporation time, substrates which had 3 different temperatures were used, sample 4a, 4b and 4c as shown in Table 1. From this experiment, quite different cracked patterns by the condition were observed as shown in Figure 15 (a) from room temperature substrates and (b) for 60°C substrate temperatures. The patterns from sample 4b were categorized between these two representative patterns. Circular light interference fringes are evident within the separated film section in Figure 15(b), caused by partial separation from the substrate.

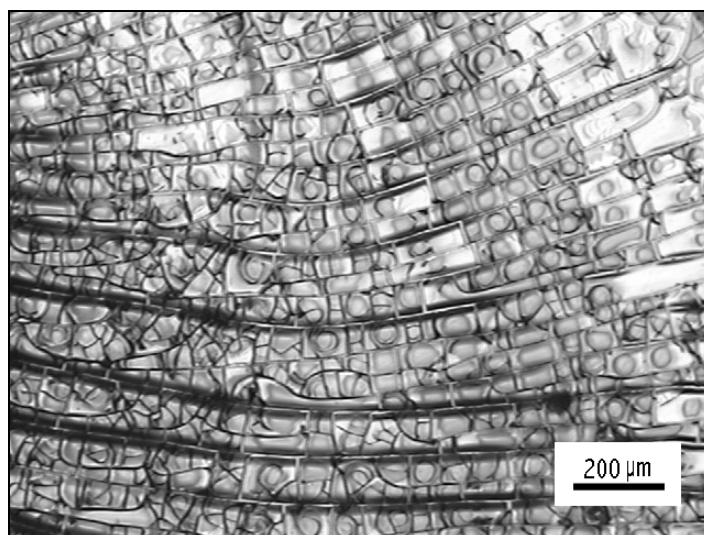


(a)

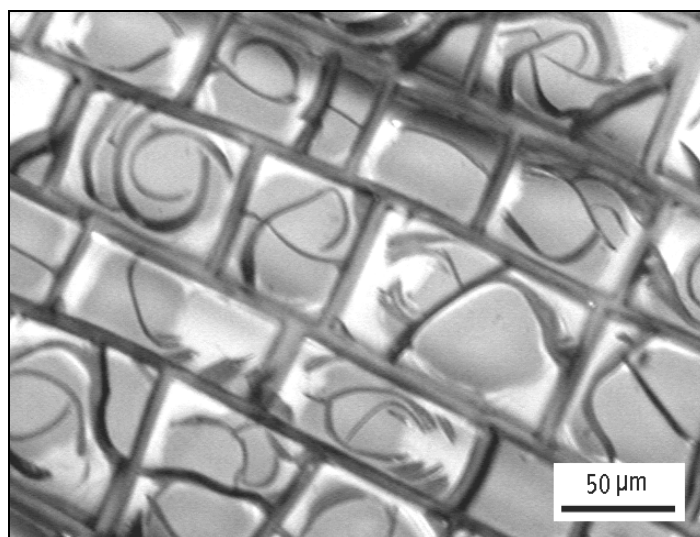


(b)

Fig. 13. (a) Polarized optical microscopic image of uniform 2-D contraction separation of solution cast dendrimer films on a glass substrate, sample No. 4 (1.0 wt%). (b) High magnification, unpolarized image of same sample.

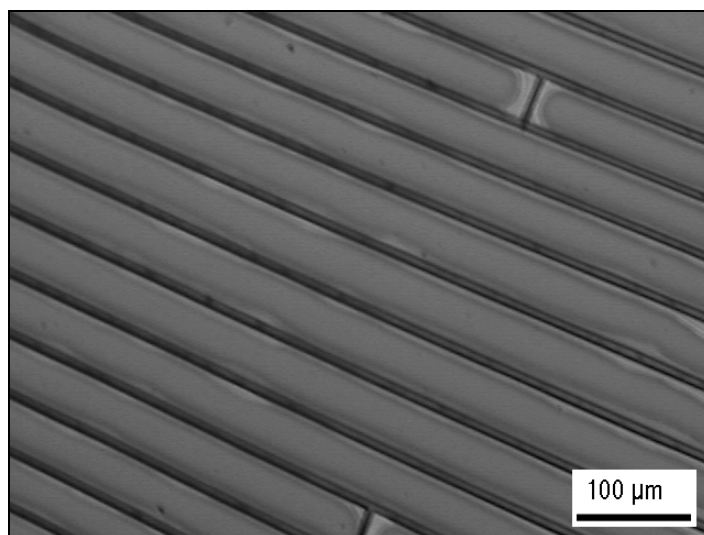


(a)

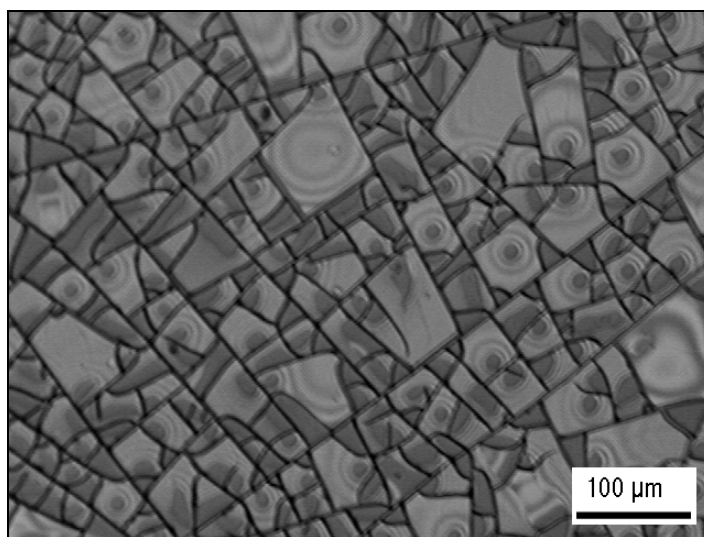


(b)

Fig. 14. (a) Irregular crack propagation within the regularly structured blocks of the solution cast film with a high concentration of dendrimer, sample No. 5 (2.0 wt%). (b) High magnification image of the same sample.



(a)



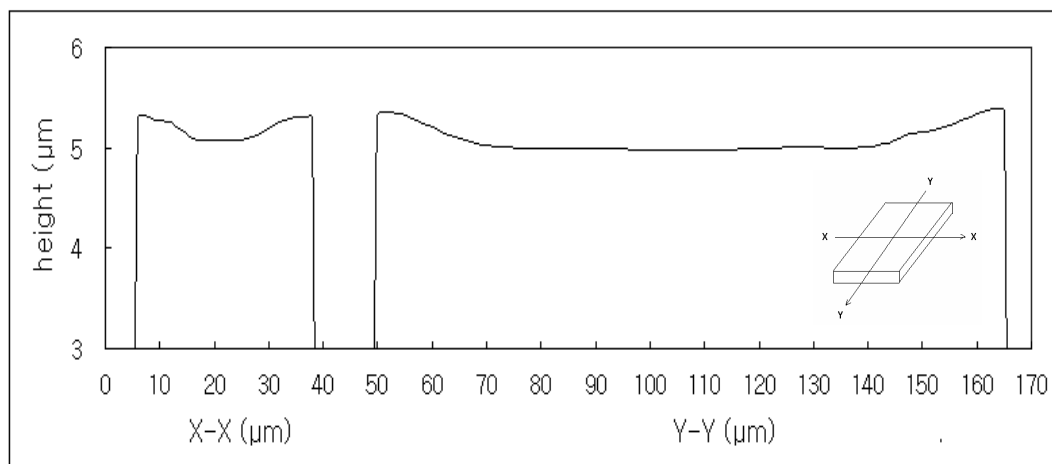
(b)

Fig. 15. Optical micrographs of difference of contraction separation patterns due to the temperature effect over solution cast films. (a) Sample No. 4a, (1.0 wt%) at 25°C, (b) sample No. 4c (1.0 wt%) at 60°C.

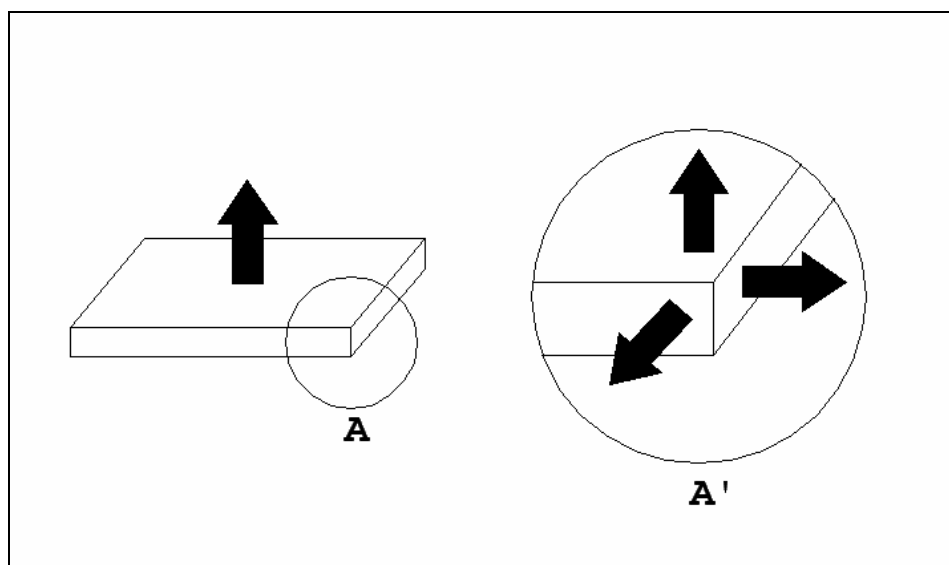
3.3.2 Surface Profile and Thickness Variation in The Region of Regularly Structured Area in The Dendrimer Cast Film

With the dendrimer cast films from the sample 3, 4, and 5 surface profile measurements were conducted for thickness variation in the region of the uniformly structured areas. For a single block, the thickness along the edges where the contraction separation occurred is generally 10 to 15% thicker than that of the middle area, hence in the cross-sectional view of the single block, the profile of top surface of each block shows a profile of similar to that of a concave lenses. See Figure 16. This observation suggests the separated blocks curl into a concave geometry as a result of separation of the block from the substrate at the block periphery.

For the surface profile on a larger scale, the thickness of the regular structured blocks which were located in various areas in a single film were deliberately measured and plotted against the radius of the whole cast film, Figure 17 (a). The thickness of the whole film area decreases with increasing radius as expected. This shows that a higher number of dendrimer molecules are accumulated near the center area of the films. In Figure 17 (b), the white arrow represents the direction of X axes in Fig. 17 (a). As radius in X axes decreases, means nearer the center of the films, the irregularity of contraction separation pattern increases.

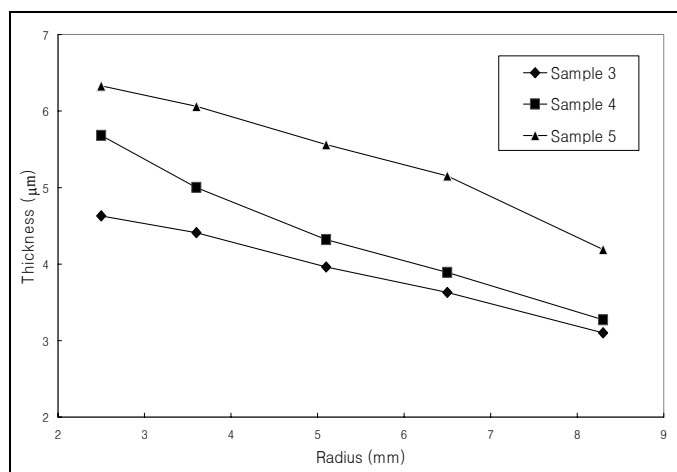


(a)

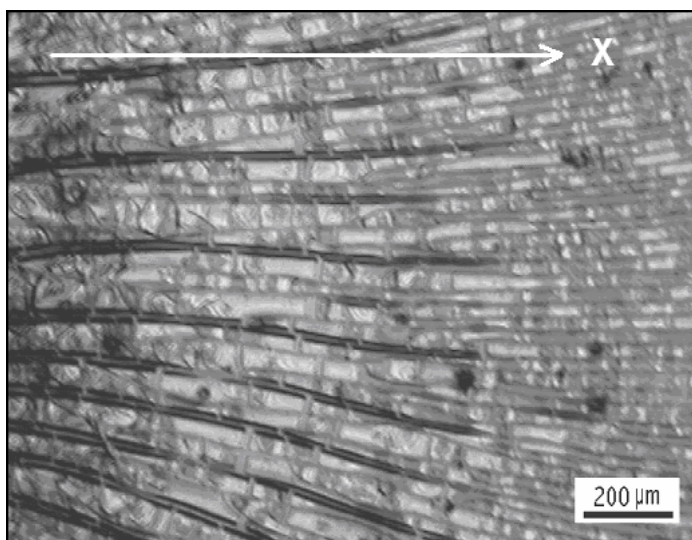


(b)

Fig. 16. (a). Surface profile of a regularly separated single block, sample No. 3 (0.8 wt%). (b) Illustration of comparison of the solvent evaporation sites.



(a)



(b)

Fig. 17. (a) Surface profile of solution cast thin film of melamine based generation 3 dendrimer, sample No. 3 (0.8 wt%), 4 (1.0 wt%), and 5 (2.0 wt%), (b) near the center, irregularity of cracking behavior is higher than periphery of cast film, sample No. 5 (2.0 wt%).

3.3.3 Small Angle X-ray Scattering (SAXS)

With the films which were cast from sample No 3 and 4a, small angle X-ray scattering (SAXS) and transmission electron microscope (TEM) electron scattering tests were performed to detect diffraction or scattering due to the regularly ordered structure in 3-D. However, no scattering and/or diffraction event was observed from these experiments. From this result, it is evident that even showing the regular contraction separation phenomenon, the dendrimer films don't develop 3-D ordered structure during solvent evaporation.

3.4 Discussion

3.4.1 Uniform 2-D Contraction Separation Phenomena of Solution Cast

Dendrimer Films

The same pattern of regular separation contractions were observed on every substrate which was used in this experiment, i.e. glass, aluminum, copper, and polyethylene film. However, the separation contraction patterns varied with the concentrations of each sample on the different substrates. From these results, it might be stated that the tendency to exhibit the pattern of regular contraction separation is not dependent on the interface between dendrimer film and the substrate, but rather the

concentration of dendrimer/chloroform solution, and the total number of dendrimer molecules which are accumulated on the surface of the substrates.

In this study, we also describe the dynamics of film formation which depend on the concentration of the dendrimer solution and the spherical nature of the dendrimer molecular structure. At the first stage of film formation the surface energy of the dendrimer molecules drives structural order due to ionic surface aggregation of the dendrimer molecules [21, 22]. This driving force seems to lead to self-assembly of molecules. In the second stage of evaporation and film contraction, adhesion strength between the cast film and the substrate as well as 2-D stresses between dendrimer molecules causes separation where the stress due to contraction is stronger than the adhesion strength between a film and substrate.

In the macroscopic view, the contraction separation process can be divided into two steps. As shown in Figure 18 (a), due to contraction stress in the tangential direction of the film, separations which are aligned in the radial direction develop in advance of the tangential direction separations which are induced by radial shrinkage, (Figure 18 (B)). Within these contraction separation phenomena, mobility of dendrimer molecules which arises because of the spherical nature of the molecules of the same size, induces macroscopic reorientation and a change in molecular configuration under the contraction stress. The effects of reorientation are exhibited as a form of large scale geometric regularity.

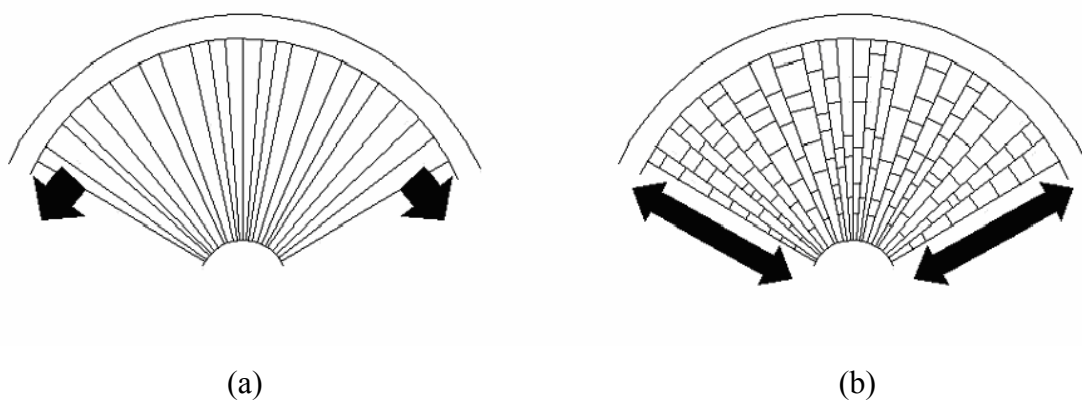


Fig. 18. Schematic representation of contraction separation in solution cast film. Discontinuity of tangential separation explains that contraction separation developed in (a) radial direction prior to (b) tangential separation.

3.4.2 Surface Profile and Thickness Variations

For a single block of the regularly separated cast film, as shown in Figure 16(a), the middle region is thinner and/or remains bonded to the substrate than the edges where the block to block separation occurred. Greater solvent evaporation occurs at block edges because there are free surfaces in three dimensions. Figure 16(b) is an illustration of solvent evaporation sites. Black arrows represent the solvent evaporation.

As we can see in the left figure, at the center of the block, solvent evaporation can occur only in 1 direction, however at the edge where block to block separation occurred, 2-D or 3-D solvent evaporation is possible, as in the right figure. This multi-free surface solvent evaporation induces greater shrinkage at the edge regions than at the block centers, which eventually leads to block edge separation from substrate and 2-D curling of the free film area.

However, the center of the block does not separate from substrate because it is not exposed to such high shrinkage stresses at the substrate-film surface. Slower diffusion of solvent at the center region allows relaxation of shrinkage stresses while film is still soft, and, hence, film separation from the substrate does not occur.

For the larger scale surface profile of the cast dendrimer films, shown in Figure 17, the center area of the whole film is thicker than the periphery of the film. This means that more dendrimer molecules accumulated in the central area of the film. During the room temperature solvent evaporation process, film solidification during solvent evaporation occurs initially at the periphery and moves toward center region.

The block separation patterns near the center area of sample No. 4 exhibited a higher irregularity in film separation.

From the observation stated above, microcracking sequences can be summarized as followings. As the solvent on the substrate evaporates, the film solidification is initiated and propagated from periphery toward the center region of a droplet. At the beginning stage of solidification, radial cracks occur ahead of tangential ones. Hence, the development of a regular cracking pattern is dominant in the film periphery area. However, in the center region, the magnitude of tangential and radial shrinkage stresses become similar to each other, hence, both directional cracks develop simultaneously and irregular cracking patterns are dominant in the center and near-center regions.

In summary, at a macroscopic level of regular rectangular block pattern formation, at the exterior block edges, where block to block separations occur, separations in radial direction develop prior to those in tangential direction at the periphery of the cast film. At interior area, due to relatively slower solidification, separations in both radial and tangential directions occur in a similar time frame. At a microscopic level, separated block shrinkage is affected by the solvent evaporation rate. At the edge of blocks, due to relatively fast three dimensional solvent evaporation rate, compared to interior of the block, film separation from substrate and curling of block surface occur.

CHAPTER IV

THERMAL PROPERTIES OF MELAMINE BASED DENDRIMER NANOPARTICLE

4.1 Introduction

Chapter IV is composed of two different experiments which describe thermal properties of melamine based, generation 3 dendrimers. The first part is carried out using the differential scanning calorimetry (DSC) with the samples which are either powders or solution cast films. The results from the DSC tests were plotted and compared to the result of polypropylene samples. The second part of Chapter IV addresses the utilization of atomic force microscopy (AFM) studies of solution cast, annealed dendrimer films. The observation from AFM studies are discussed and compared with the results of Chapter III.

4.2 Experimental

4.2.1 Differential Scanning Calorimetry (DSC)

Conventional differential scanning calorimetric (DSC) analysis and dynamic differential scanning calorimetric (DDSC) analysis were conducted using a Perkin-Elmer DSC Pyris 1 Series Thermal Analysis System. Two different phases of the same

dendrimer samples were prepared for the DSC tests. One was in powder form and the other was a film sample which was directly cast into the DSC sample pan. The DSC sample preparation for the cast film was the same as that of sample no.4, shown in Table 1. After the dendrimer-chloroform solution which had the same concentration with sample no.4 was prepared, the solution was dripped directly on the DSC 50 ml sample pan, and allowed to dry. At the same time, another sample pan was prepared for the DSC reference pan, on which pure chloroform was dripped and evaporated completely. All sample preparation steps were carried out at room temperature. DSC analyses were carried out from 0 to 300°C with a heating rate of 15.0°C/min; DDSC analyses were performed from 25°C to 275°C with heating and cooling rates of 10 and 5°C/min respectfully. DSC analyses were carried out under a nitrogen atmosphere.

4.2.2 Atomic Force Microscopy (AFM)

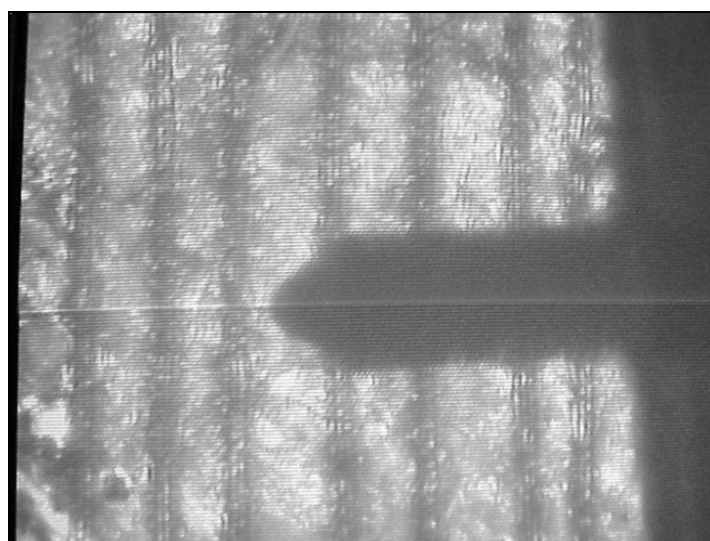
For the atomic force microscopy, G3D dendrimer samples were prepared as followed. The solution concentrations for all samples used in this AFM experiment were fixed at 1.0 wt%, and the substrate temperatures were room temperature. All conditions of samples were the same as sample no. 4a, listed in Table 1. As observed and stated in Chapter III, the contraction separation patterns didn't show any difference by the choosing of substrate material, all the samples for AFM tests were cast on the iron AFM sample plates directly from solutions.

All AFM tests were carried out on a Digital Instruments Nanoscope AFM/STM for scanning probe microscopy. The system comprises of a Nanoscope III controller fitted to a MultiMode TM scan head. The test mode of AFM was in the tapping mode, where the cantilever oscillation amplitude variation is monitored, which is caused by the interaction of the tip with the sample surface. A silicon cantilever (length 125 μm , width 30 μm , thickness 3-5 μm) was used with a spring constant between 17 and 64 N/m and a resonance frequency in air of an amplitude of about 10-20 nm. Imaging was performed by displaying the height signal.

The 1.0 wt% sample solution was cast on the iron AFM sample plate and dried at room temperature. After solvent was evaporated from the solution cast dendrimer film on the iron plate, it was placed in the AFM sample holder and examined. As AFM is non-destructive test, after the samples were examined by AFM, they were placed in the vacuum oven, at 100°C, and annealed for 2 hours. The annealed samples were reexamined by AFM and the data from both before and after annealing were compared. The AFM microscopy system is shown in Figure 19(a) and screen image of the scanning cantilever on a cracked dendrimer film is shown in Figure 19(b).



(a)



(b)

Fig. 19. (a) Digital Instruments Nanoscope AFM/STM for scanning probe microscopy system. (b) Monitor screen image of scanning cantilever on a regularly cracked dendrimer film sample, (Tip Width $\sim 80\mu\text{m}$).

4.3 Results

4.3.1 Thermal Properties of Melamine Based Generation 3 Dendrimer from DSC

It is well known that dendrimers have different physio-chemical properties compared with linear structured polymers because of their molecular architecture [10]. In this study, the thermal properties of newly synthesized melamine based generation 3 dendrimer were determined from conventional and dynamic DSC measurements. The samples for both were prepared in the form of either a white powder or a cast film from the solution of sample 4. The thermal properties of melamine based generation 3 dendrimers are listed in Table 2 and the DSC curves of both samples are compared in Figure 20 in which a weak second order transition (T_1) is detected at 69°C with an apparent endothermic melting point near 240°C.

4.3.2 Atomic Forced Microscopy (AFM) Results with Annealed Dendrimer Thin Films

The selected image from the AFM test with G3D dendrimer film, which was cast from their solution having concentration 1.0 wt%, before annealing at 100°C for 2 hours is shown below in Figure 21. The data ranges in X-Y plane are 200nm × 200nm, and maximum scale in Z-direction is within ± 2.5 nm. Figure 22 (a) is the result image of sample dendrimer film after 2 hours annealing at 100°C in a vacuum oven.

Table 2.

Thermal properties of melamine based dendrimers determined by DSC.

Sample Type	T ₁ (°C)	T _m (°C)	T ₁ (°K)/T _m (°K)	ΔH(J/g)
Cast Film	69	242.7	0.66	38.628
Powder	69	238.7	0.67	8.889

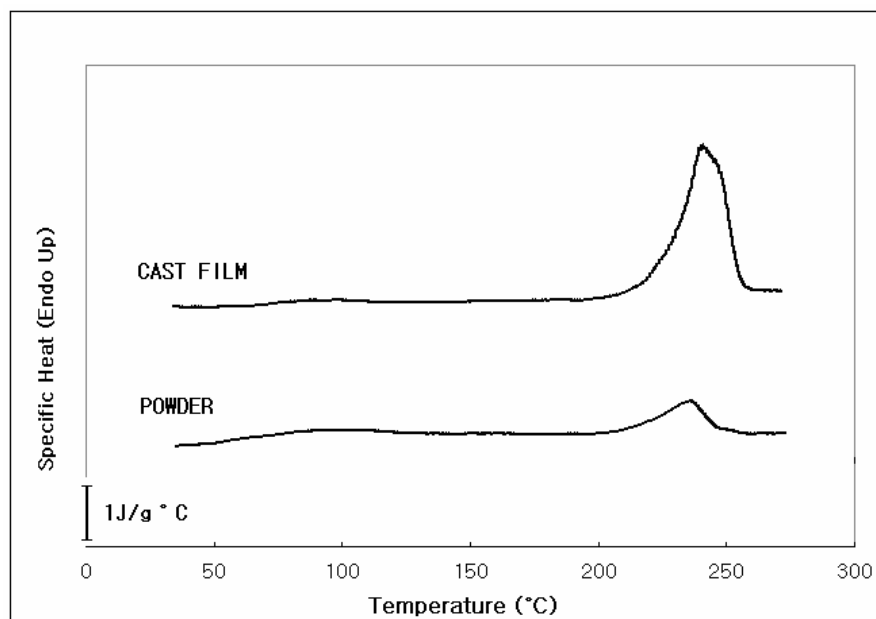


Fig. 20. DSC curves of melamine based dendrimers in powder and cast film. The cast film curve is shifted vertically.

When it was compared with the image in Figure 21, it is evident the annealed film exhibited a smoother surface after annealing.

One interesting phenomenon was also observed in Figure 22 (a). As we can see from the image, there was abrupt height change on the surface of the annealed dendrimer film and these were found from all annealed samples. The average of number of troughs are 15 ± 3 from all scanned sample with scanning area of $5 \mu\text{m} \times 5 \mu\text{m}$. Each trough has various shapes and sizes, however, the height of each step of all troughs are approximately 2.4nm. Figure 22 (b) is a cross sectional image of A-A on an image in Figure 22 (a). As shown in Figure 22 (b), Δh is the average trough height difference between adjacent terraces, approximately 2.4nm.

4.4 Discussion

4.4.1 Thermal Properties of Melamine Based Generation 3 Dendrimer

From the DSC tests, weak transition temperatures (T_1) of generation 3 melamine based dendrimers in the forms of both powder and a cast film were observed at 69°C . On an absolute temperature scale, glass transition temperatures are generally between 0.6 and 0.7 of the melting point [49, 50]. According to this scale, the measured transition temperature, 69°C (342°K) is 0.67 of measured melting temperature, 240°C (513°K). Hence there is a possibility that the glass

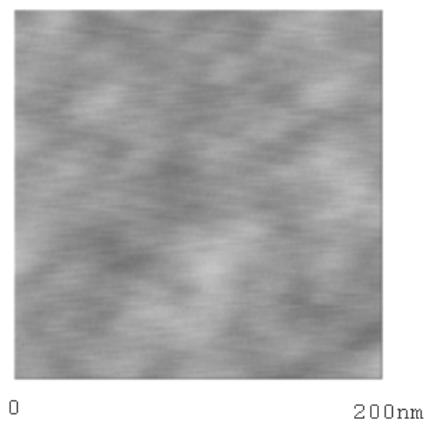


Fig. 21. AFM result image from solution cast G3D dendrimer film before annealing. Maximum data scale in Z-direction is $\pm 2.5\text{nm}$.

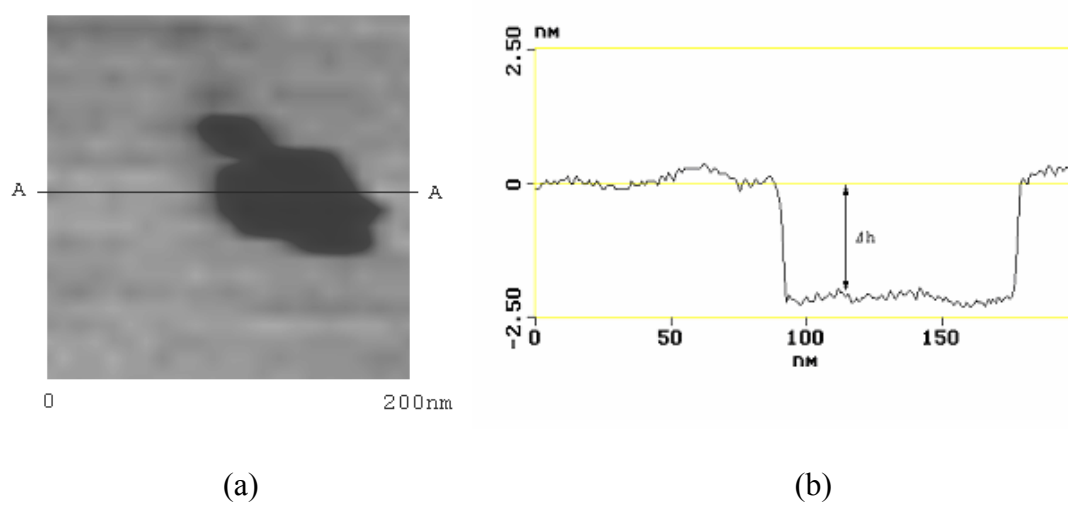


Fig. 22. (a) AFM result image from solution cast G3D dendrimer film after annealing (100°C , 2 hours). Maximum scale in Z-direction is $\pm 2.5\text{nm}$. (b) Cross sectional view of A-A on image (a).

transition temperature (T_g) of the melamine based generation 3 dendrimer might be in the similar range with T_1 .

From studies to date, dendrimers do not crystallize and do not exhibit a melting temperature (T_m) in their thermal properties. However, in this study, the sample material, melamine based generation 3 dendrimer, showed melting-like behavior at around 240°C during the DSC test and at 275°C , this material starts to decompose. By calculating the areas under the peaks of DSC curves, the specific heats of each sample were determined. As shown in Table 2, and Figure 6, the amount of specific heat at the quasi-melting peak of the cast film sample is 4.35 times greater than that of powder sample. The cast film samples are prepared by solution casting directly onto the DSC sample pan, the dendrimer molecules evidently form more regular structures from the solvent casting process.

Depolarization of the polarized light by the middle area of the cast film blocks due to the stress induced orientation is shown in Figure 13 (a) and in Figure 23 at higher magnification. To dissociate this regular structure the cast film samples need more energy than the powder samples which are less well-ordered after their synthesis.

4.4.2 Atomic Forced Microscopy (AFM) Results with Annealed Dendrimer Thin Films

From comparison between the AFM data images of solution cast dendrimer films both before and after annealing, as shown in Figure 21 and 22 (a), the surface of

the annealed film exhibits less rough and a smoother surface topography. This observation indicates that the annealing process enhances the molecular packing of the dendrimer so as to be packed more closely with a higher regularity. In Figure 24, we illustrate a schematic model of ideally cross-packed molecular balls in thin films on a substrate. As already known, generation 3 dendrimers have an elliptic cross sectional shape rather than perfect sphere form [3]. Based on this elliptic sphere geometry and the dendrimer sizes modeled and measured by Simanek et al [48], the ideal schematic model of close-packed molecules is illustrated in Figure 24.

In this model, the thickness of a layer would be approximately 2nm, as shown as Δh in Figure 24. The AFM observed Δh , trough depth in Figure 23 (b) can be associated with the thickness of a single layer of dendrimers [51, 52]. This also reflects a high structural regularity of the dendrimer molecules in the first monolayer in solution cast films.

Even with SAXS and TEM, any evidence of highly ordered structure was not found from the cast dendrimer films, however, a possibility of structural regularity of dendrimer molecules in the cast film was allowed from the observed AFM data and ideal structure model.

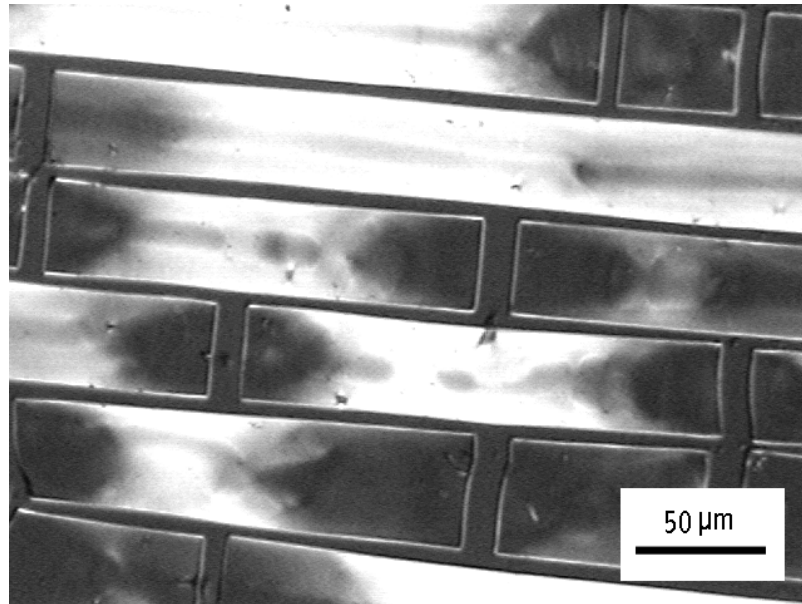


Fig. 23. Polarized light image of sample No. 4 (1.0 wt%). The bright areas exhibit birefringence under the polarized light from the light source due to the stress-induced order.

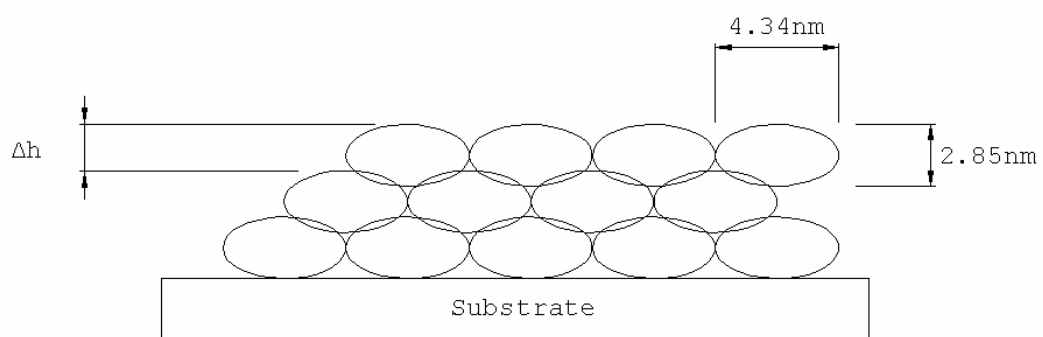


Fig. 24. An ideal schematic model of close packed elliptic sphere molecules on a substrate. Δh represents the thickness of first monolayer.

CHAPTER V

CONCLUSIONS

5.1 Primary Findings

In this study, several physical properties, including regular microcrack development from casting thin films and thermal properties of melamine based, generation 3 dendrimer in the form of powder and solution cast thin film were investigated in order to observe any structural order at the microscopic and macroscopic ranges. The ultimate aim of this study was to ascertain whether dendrimers, as one of spherically structured nano-scale particles can become ordered into a self-assembled regular structure due to the nature of their regular sizes and shapes.

This study observed and described the unique phenomenon of regular contraction separation of solution cast film made from generation 3 melamine based dendrimers and thermal properties, such as glass transition temperature (T_g) and melting temperature (T_m) of the dendrimer itself.

Solution cast films of synthesized [48] melamine based generation 3 dendrimers exhibit unique microcrack contraction separation phenomena when solution cast as films. The cast films from a concentration of around 0.8 wt% and higher exhibit regular 2-D separation contraction and form well developed regularly arrayed structures due to the sequence of radial and tangential crack development. Both powder and cast film samples show similar apparent melting behavior with the cast film exhibiting a larger

endotherm in DSC, indicating a greater degree of order. The cast film samples require more energy for structure disruption than powder samples. However, no ordered regions were observed by small angle X-ray scattering (SAXS) and transmission electron microscopy (TEM).

The results from AFM tests with the solution cast dendrimer films both before and after annealing indicates that the favorable conditions, i.e., enough time and mobility can help dendrimer molecules to be self-assembled and have a regular structure. The thickness of first monolayer troughs (similar to metal dislocations) of self-assembled solution cast dendrimer film suggests structural regularity of the dendrimer molecules after the annealing process for the exterior film layers. Based on these AFM observations, the physical structure model of annealed dendrimer cast film was established in Figure 24. This model was also compared with the sizes of the computer program generated model of single dendrimer molecule with the lowest energy level in Figure 10 (b).

5.2 Suggestions for Future Research

In view of the fact, dendrimers have the potential to self-assemble for a high structural regularity due to their homogeneity in sizes and shapes is shown. Achievement of high structural regularity in the nanometer range is expected to make it possible for us to utilize dendrimers for many applications, for example, lighter but

higher capacity batteries, better performance catalyst membranes, and electronic packaging.

To verify and apply the properties of the nanometer-range structural regularity of dendrimers, we need to develop and utilize more stiff spheres which can maintain their sizes and shapes that would assist self-assembly. The stiffness of dendrimer material can be achieved by either synthetic methods or functionalization after synthesis using metal ions, such as Li^+ ions. Moreover, surface functionalized dendrimers would favor self-assembly.

REFERENCES

1. Fischer M, Vögtle F. *Chem, Int Ed Engl* 1999; 38: 884.
2. Mitsutoshi JM, Kakimoto M. *Prog Poly Sci* 2001; 26: 1233.
3. Marcel HP, Genderen V, Meijer EW, Reinhoudt DN. *Supramolecular materials and technologies, Prospectives in supramolecular chemistry, Vol 4*, New York: John Wiley & Sons Ltd., 1999.
4. Tomalia DA, Majoros I, Ciferri A. *Supramolecular polymers*, New York: Marcel Dekker, Inc., 2000.
5. Dvornic PR, Leuze-Jallouli AM, Owen MJ, Perz S. *J Am Chem Soc*, 1998; 120:473.
6. Patri AK, Majoros I, Baker JRJ. *Current Opin In Chem Biol* 2002; 6: 466.
7. Bar-Haim A, Klafter J. *J. Luminescence* 1998; 76 & 77: 197.
8. Dvornic PR, Leuze-Jallouli AM, Owen MJ, Perz S. *J Am Chem Soc* 2000; 122: 241.
9. Leuze-Jallouli AM, Swanson D, Dvornic PR, Perz SV, Owen M. *J Am Chem Soc* 1997; 118: 93.
10. Dvornic PR, Leuze-Jallouli AM, Owen MJ, Dalman DA, Parham P, Pickelman D, Perz V. *J Am Chem Soc* 1999; 121: 187.
11. Burn PL, Beavington R, Frampton MJ, Pillow JNG, Halim M, Lupton JM, Samuel IDW. *Mater Sci Eng B* 2001; 85: 190.
12. Zhao Y-L, Cai Q, Jiang J, Shuai X-T, Bei J-Z, Chen C-F, Xi F. *J Polymer* 2002; 43: 5819.
13. Vogit-Martin, IG, Garbella RW, Schumacher M. *Macromolecules* 1992; 25: 961.

14. Buchko CJ, Wilson PM, Xu Z, Zhang J, Moore JS, Martin DC. *J Polymer* 1995; 36: 1817.
15. Tokuhisa H, Zhao M, Baker LA, Phan VT, Dermody DJ, Garcia ME, Peez RF, Crooks RM, Mayer TM. *J Am Chem Soc* 1998; 120: 4492.
16. Diaz DJ, Storrer GD, Bernhard S, Takada K, Abruna HD. *Langmuir* 1999; 15: 7351.
17. Cheng L, Cox JA. *J Electrochem Comm* 2001; 3: 285.
18. Liu T, Burger C, Chu B. *J Prog Polym Sci* 2003; 28: 5.
19. Hernandez-Lopez JL, Bauer RE, Chang WS, Glasser G, Grebel-Koehler D, Klapper M, Kreiter M, Leclaire J, Maajoral JP, Mittler S, Mullen K, Vasilev K, Weil T, Wu JT, Knoll WJ. *Mater Sci Eng* 2003; C23: 267.
20. Buleier E, Wehner W, Vogtle F. *Synthesis* 1978; B34: 155.
21. Steed J, Atwood J. *Supramolecular chemistry*, New York: John Wiley & Sons Ltd. 2000.
22. Tomalia DA, *J Polymer* 1985; 12(1): 117.
23. Flory PJ. *J Am Chem Soc* 1941; 63: 3083.
24. Flory PJ. *J Am Chem Soc* 1941; 63: 3091.
25. Flory PJ. *J Am Chem Soc* 1941; 63: 3096.
26. Flory PJ. *Principles of polymer chemistry*, New York: Cornell University Press, 1953.
27. Flory PJ. *J Am Chem Soc* 1952; 74: 2718.
28. Maciejewski M. *J Macromol Sci Chem* 1982; A17: 689.
29. Newkome GR, Yao Z, Baker GR, Gupta VK. *J Organ Chem* 1985; 50: 2004.

30. Newkome GR, Yao Z, Baker GR, Gupta VK, Russo PS, Saunders MJ. *J Am Chem Soc* 1986; 108: 849.
31. Newkome GR, Baker GR, Saunders MJ, Russo PS, Gupta VK, Yao Z, Miller JE, Bouillion K. *J Chem Soc, Chem Commun* 1986; 107: 752.
32. Tomalia D, Baker H, Dewald J, Hall M, Kallog G, Martin S, Roeck J, Ryder J, Smith P. *J Polymer* 1985; 17: 117.
33. Hobson L, Feast W, *J Polymer* 1999; 43: 1279.
34. Tomalia DA, Berry V, Hall M, Hedstrand DM. *Macromolecules* 1987; 20: 1164.
35. Tomalia DA, Naylor AM, Goddard WAI. *Angew Chem Int Ed Engl* 1990; 29: 138.
36. Frechet J, Hawker C. *J Am Chem Soc* 1990; 112: 7638.
37. Watkins DM, Sweet YS, Kimash JW, Turro NJ, Tomalia DA. *Langmuir* 1997; 13: 3136.
38. Matthews OA, Shipway AN, Stoddart JF. *Prog Polym Sci* 1998; 23: 1.
39. Zhao M, Sun L, Crooks RM. *J Am Chem Soc* 1998; 120: 4877.
40. Kopelman R, Shortreed M, Shi ZY, Tan W, Xu Z, Moore JS, Bar-Haim A, Klafter J. *Phys Rev Lett* 1997; 78: 1239.
41. Jansen JF, Brabander-van DBGA, Meijer EW. *Science* 1997; 266: 1226.
42. Lakowski WM, Ghosh P, Crooks RM. *J Am Chem Soc* 1999; 121: 1419.
43. Tully DC, Wilder K, Frechet J, Trimble A, Quate C. *Adv Mater* 1999; 11: 314.
44. Haines P. *Thermal methods of analysis*, 1st Ed., London: Blackie Academic and Professional, 1995.

45. Young RJ, Lovell PA. Introduction to polymers, 2nd Ed., New York: Chapman and Hall, 1991.
46. Binnig G, Quate CF, Gerber CH. Phys Rev Lett 1989; 56(9): 930.
47. Meyer E. Prog Surf Sci 1992; 41: 3.
48. Zhang W, Nowlan DT III, Thomson LM, Lackowski WM, Simanek EE. J Am Chem Soc 2001; 123: 8914.
49. Lee WA, Knight GJ. J Chem Phys 1970; 43: 139.
50. Morgan RJ, Nielsen LE. J Pol Sci 1972; 10: 1575.
51. Stocker W, Schurmann BL, Rabe JP, Forster S, Lindner P, Neubert I, Schluter AD. Adv Mater 1998; 10: 793.
52. Keller DJ, Chih-Chung C. Surf Sci 1992; 268: 333.

VITA

Woong Jae Boo received his B.S degree in mechanical engineering from Hankook Aviation University (Republic of Korea) in February 1995. He received his M.S degree in mechanical engineering from Texas A&M University (College Station, Texas, USA) in December 2003 under the guidance of Dr. Roger J. Morgan. His permanent address is 207-1203 Jukong, Daebang-dong, Dongjak-ku, Seoul, Korea.